Electron-impact ionization of Li_2 using a time-dependent close-coupling method

M. S. Pindzola, Sh. A. Abdel-Naby, J. A. Ludlow, and F. Robicheaux
Department of Physics, Auburn University, Auburn, Alabama 36849, USA

J. Colgan
Theoretical Division, Los Alamos National Laboratory, Los Alamos, New Mexico 87545, USA

(Received 21 June 2011; revised manuscript received 29 November 2011; published 17 January 2012)

The time-dependent close-coupling method is applied to calculate the electron-impact ionization of a diatomic molecule with interior closed subshells. The ionization of the outer $2s\sigma$ subshell of $Li_2(1s\sigma^2 2p\sigma^2 2s\sigma^2)$ is carried out using a standard core orthogonalization method. At the peak of the Li_2 cross section, the nonperturbative time-dependent close-coupling cross sections are found to be lower than perturbative distorted-wave cross sections. The reductions due to electron correlation effects are in keeping with previous reductions of peak cross sections seen in the electron-impact ionization of neutral atoms.

DOI: 10.1103/PhysRevA.85.012704 PACS number(s): 34.80.Dp, 34.80.Gs

I. INTRODUCTION

Studies of the electron-impact ionization of diatomic molecules at low incident energies probe the quantal dynamics of two continuum electrons moving in the nonspherical Coulomb field of the molecular core. To date, nonperturbative theoretical methods which treat correlation effects for the two slow-moving continuum electrons have been limited to the ionization of H_2^+ and H_2. The R-matrix-with-pseudostates method has produced total cross sections for the electron-impact ionization of H_2 [1] that are in good agreement with H_2 experiments [2,3] in the near threshold region. The time-dependent close-coupling method has produced total cross sections for the electron-impact ionization of H_2^+ [4] and H_2 [5] that are in good agreement with H_2^+ experiments [6] and H_2 experiments [2,3] over a wide energy range. More recently [7,8], the time-dependent close-coupling method has been used to calculate energy and angle differential cross sections for the electron-impact ionization of H_2 and compared with three-body distorted-wave calculations and experiment.

To perform time-dependent close-coupling calculations for the electron-impact ionization of diatomic molecules beyond H_2^+ and H_2, we need a method that prevents overoccupation of filled subshells during the time evolution of the close-coupled equations. In this article, we apply a standard core-orthogonalization method to allow time-dependent close-coupling calculations to be carried out for the electron-impact ionization of any diatomic molecule. Our first application is to the electron-impact ionization of the $2s\sigma$ subshell of $Li_2(1s\sigma^2 2p\sigma^2 2s\sigma^2)$. To check the time-dependent close-coupling results for Li_2, we adapt a previously developed configuration-average distorted-wave method [9] to make calculations using the same ionized subshell orbital and core scattering potential as used in the time-dependent close-coupling calculations.

The rest of the article is organized as follows: Formulations of the time-dependent close-coupling and configuration-average distorted-wave methods are given in Sec. II, electron-impact ionization cross sections for Li_2 are presented in Sec. III, and a brief summary is given in Sec. IV. Unless otherwise stated, all quantities are given in atomic units.

II. THEORY

A. Time-dependent close-coupling (TDCC) method

The time-dependent Schrödinger equation for electron scattering from one active electron in a homonuclear diatomic molecule is given by

$$i\frac{\partial\Psi(\vec{r}_1,\vec{r}_2,t)}{\partial t} = H(\vec{r}_1,\vec{r}_2)\Psi(\vec{r}_1,\vec{r}_2,t), \tag{1}$$

where the nonrelativistic Hamiltonian is given by

$$H(\vec{r}_1,\vec{r}_2) = \sum_{i=1}^{2}\left(-\frac{1}{2}\nabla_i^2 - \sum_{\pm}\frac{Z}{\sqrt{r_i^2+\frac{1}{4}R^2 \pm r_i R\cos\theta_i}} + V_{HX}(r_i,\theta_i)\right) + \frac{1}{|\vec{r}_1-\vec{r}_2|}, \tag{2}$$

where Z is the charge on each nucleus, R is the internuclear distance, and $V_{HX}(r,\theta)$ is a Hartree with local exchange potential. Expanding the total wave function in products of rotational functions and substitution into Eq. (1) yields a set of time-dependent close-coupled equations for each MS symmetry given by [10]

$$\begin{aligned} i\frac{\partial P^{MS}_{l_1 l_2}(r_1,\theta_1,r_2,\theta_2,t)}{\partial t} &= T_{m_1 m_2}(r_1,\theta_1,r_2,\theta_2)P^{MS}_{m_1 m_2}(r_1,\theta_1,r_2,\theta_2,t) \\ &\quad + \sum_{m_1',m_2'} V^{M}_{m_1 m_2, m_1' m_2'}(r_1,\theta_1,r_2,\theta_2)P^{MS}_{m_1' m_2'}(r_1,\theta_1,r_2,\theta_2,t). \end{aligned} \tag{3}$$

The total one-body operator is given by

$$\begin{aligned} T_{m_1 m_2}(r_1,\theta_1,r_2,\theta_2) &= \sum_{i=1}^{2}\left(K(r_i) + \bar{K}(r_i,\theta_i) + \frac{m_i^2}{2r_i^2\sin^2\theta_i}\right) \\ &\quad + \sum_{i=1}^{2}\left(-\sum_{\pm}\frac{Z}{\sqrt{r_i^2+\frac{1}{4}R^2 \pm r_i R\cos\theta_i}} + V_{HX}(r_i,\theta_i)\right), \end{aligned} \tag{4}$$

where $K(r)$ and $\bar{K}(r,\theta)$ are kinetic energy operators. The two-body operator is given by

$$V^{M}_{m_1m_2,m_1'm_2'}(r_1,\theta_1,r_2,\theta_2) = \sum_{\lambda} \frac{(r_1,r_2)^{\lambda}_{<}}{(r_1,r_2)^{\lambda+1}_{>}} \sum_{q} \frac{(\lambda-|q|)!}{(\lambda+|q|)!} P^{|q|}_{\lambda}(\cos\theta_1) P^{|q|}_{\lambda}(\cos\theta_2)$$
$$\times \int_0^{2\pi} d\phi_1 \int_0^{2\pi} d\phi_2 \Phi_{m_1}(\phi_1)\Phi_{m_2}(\phi_2) e^{iq(\phi_2-\phi_1)} \Phi_{m_1'}(\phi_1)\Phi_{m_2'}(\phi_2), \tag{5}$$

where $P^{|q|}_{\lambda}(\cos\theta)$ is an associated Legendre function and $\Phi_m(\phi) = \frac{e^{im\phi}}{\sqrt{2\pi}}$ is a rotational function.

The initial condition for the solution of the TDCC equations for the ionization of the $2s\sigma$ subshell of $Li_2(1s\sigma^2 2p\sigma^2 2s\sigma^2)$ is given by

$$P^{MS}_{m_1m_2}(r_1,\theta_1,r_2,\theta_2,t=0) = P_{2s0}(r_1,\theta_1) G_{k_0l_0M}(r_2,\theta_2) \delta_{m_1,0}\delta_{m_2,M}, \tag{6}$$

where $P_{nlm}(r,\theta)$ is a bound radial and angular orbital and $G_{k_0l_0m}(r,\theta)$ is a Gaussian radial and angular wave packet with incident energy $\frac{k_0^2}{2}$ and incident angular momentum l_0. Bound, $P_{nlm}(r,\theta)$, and continuum, $P_{klm}(r,\theta)$, radial and angular orbitals are obtained by diagonalization of the Hamiltonian

$$H(r,\theta) = K(r) + \bar{K}(r,\theta) + \frac{m^2}{2r^2\sin^2\theta} - \sum_{\pm} \frac{Z}{\sqrt{r^2 + \frac{1}{4}R^2 \pm rR\cos\theta}} + V_{HX}(r,\theta). \tag{7}$$

A self-consistent field molecular structure code [11,12] is used to calculate the bound radial and angular orbitals of the next higher ion stage needed to construct the $V_{HX}(r,\theta)$ potential.

To prevent collapse of the radial and angular wave functions, $P^{MS}_{m_1m_2}(r_1,\theta_1,r_2,\theta_2,t)$, into closed inner subshells during time propagation of the close-coupled equations, we use a standard core-orthogonalization method. For example, for electron-impact ionization of the $2s\sigma$ subshell of $Li_2(1s\sigma^2 2p\sigma^2 2s\sigma^2)$, the $P^{^1\Sigma}_{00}(r_1,\theta_1,r_2,\theta_2,t)$ radial and angular wave function is orthogonalized at each time step according to

$$\begin{aligned}
&\bar{P}^{^1\Sigma}_{00}(r_1,\theta_1,r_2,\theta_2,t) \\
&= P^{^1\Sigma}_{00}(r_1,\theta_1,r_2,\theta_2,t) - P_{1s0}(r_1,\theta_1)\int dr_1' \int d\theta_1' P_{1s0}(r_1',\theta_1') P^{^1\Sigma}_{00}(r_1',\theta_1',r_2,\theta_2,t) \\
&\quad - P_{2p0}(r_1,\theta_1)\int dr_1' \int d\theta_1' P_{2p0}(r_1',\theta_1') P^{^1\Sigma}_{00}(r_1',\theta_1',r_2,\theta_2,t) - P_{1s0}(r_2,\theta_2)\int dr_2' \int d\theta_2' P_{1s0}(r_2',\theta_2') P^{^1\Sigma}_{00}(r_1,\theta_1,r_2',\theta_2',t) \\
&\quad - P_{2p0}(r_2,\theta_2)\int dr_2' \int d\theta_2' P_{2p0}(r_2',\theta_2') P^{^1\Sigma}_{00}(r_1,\theta_1,r_2',\theta_2',t) \\
&\quad + P_{1s0}(r_1,\theta_1)P_{1s0}(r_2,\theta_2)\int dr_1' \int d\theta_1' \int dr_2' \int d\theta_2' P_{1s0}(r_1',\theta_1') P_{1s0}(r_2',\theta_2') P^{^1\Sigma}_{00}(r_1',\theta_1',r_2',\theta_2',t) \\
&\quad + P_{1s0}(r_1,\theta_1)P_{2p0}(r_2,\theta_2)\int dr_1' \int d\theta_1' \int dr_2' \int d\theta_2' P_{1s0}(r_1',\theta_1') P_{2p0}(r_2',\theta_2') P^{^1\Sigma}_{00}(r_1',\theta_1',r_2',\theta_2',t) \\
&\quad + P_{2p0}(r_1,\theta_1)P_{1s0}(r_2,\theta_2)\int dr_1' \int d\theta_1' \int dr_2' \int d\theta_2' P_{2p0}(r_1',\theta_1') P_{1s0}(r_2',\theta_2') P^{^1\Sigma}_{00}(r_1',\theta_1',r_2',\theta_2',t) \\
&\quad + P_{2p0}(r_1,\theta_1)P_{2p0}(r_2,\theta_2)\int dr_1' \int d\theta_1' \int dr_2' \int d\theta_2' P_{2p0}(r_1',\theta_1') P_{2p0}(r_2',\theta_2') P^{^1\Sigma}_{00}(r_1',\theta_1',r_2',\theta_2',t).
\end{aligned} \tag{8}$$

On the other hand, the $P^{^1\Pi}_{01}(r_1,\theta_1,r_2,\theta_2,t)$ radial and angular wave function is orthogonalized at each time step according to

$$\bar{P}^{^1\Pi}_{01}(r_1,\theta_1,r_2,\theta_2,t) = P^{^1\Pi}_{01}(r_1,\theta_1,r_2,\theta_2,t) - P_{1s0}(r_1,\theta_1)\int dr_1' \int d\theta_1' P_{1s0}(r_1',\theta_1') P^{^1\Pi}_{01}(r_1',\theta_1',r_2,\theta_2,t)$$
$$- P_{2p0}(r_1,\theta_1)\int dr_1' \int d\theta_1' P_{2p0}(r_1',\theta_1') P^{^1\Pi}_{01}(r_1',\theta_1',r_2,\theta_2,t). \tag{9}$$

We note that $P^{MS}_{m_1m_2}(r_1,\theta_1,r_2,\theta_2,t)$ radial and angular wave functions with $m_1 \neq 0$ and $m_2 \neq 0$ do not need to be orthogonalized.

Probabilities, $\mathcal{P}(MSl_0)$, for the electron-impact excitation and ionization processes are obtained by time propagating the close-coupled equations and then projecting the $P^{MS}_{m_1m_2}(r_1,\theta_1,r_2,\theta_2,t\to\infty)$ radial and angular wave functions onto fully antisymmetric spatial and spin wave functions constructed from bound, $P_{nlm}(r,\theta)$, and continuum, $P_{klm}(r,\theta)$, radial and angular orbitals. The probabilities are then used

to obtain total, energy differential, and energy and angle differential cross sections as a function of incident electron energy and internuclear distance [10]. For example, the total ionization cross section is given by

$$\sigma_{\rm ion} = \frac{\pi w}{4k_0^2} \sum_{M,S,l_0} (2S+1)\mathcal{P}(MSl_0), \tag{10}$$

where w is the subshell occupation number.

B. Configuration-average distorted-wave (CADW) method

Distorted-wave continuum orbitals at energies $\epsilon = \frac{k^2}{2}$ are found by solution of the single-particle Schrödinger equation given by

$$[H(r,\theta) - \epsilon]P_{klm}(r,\theta) = 0. \tag{11}$$

We solve the distorted-wave equation, including S-matrix boundary conditions, as a system of linear equations, $Au = b$ [9]. The configuration-average ionization cross section is given by

$$\sigma_{\rm ion} = \int_0^{\frac{E}{2}} d\epsilon_e \frac{64}{k_i^3 k_e k_f} \frac{w}{S(|m|)} \sum_{l_i,|m_i|} \sum_{l_e,|m_e|} \sum_{l_f} (M_d + M_e - M_x), \tag{12}$$

where the total energy $E = \epsilon_{nlm} + \epsilon_i = \epsilon_e + \epsilon_f$, $S(|m|) = 2(2 - \delta_{|m|,0})$ is the statistical weight of the nlm bound valence electron, and w is again the subshell occupation number. The direct, M_d, exchange, M_e, and cross, M_x, terms are determined using first-order perturbation theory and may be expressed in terms of weighted sums over polar coordinate Coulomb integrals [9].

III. RESULTS

Time-dependent close-coupling calculations, using the core-orthogonalization method outlined in Sec. II, were carried out for the electron-impact ionization of the $2s\sigma$ subshell of $Li_2(1s\sigma^2 2p\sigma^2 2s\sigma^2)$ at incident energies near the peak of the cross section. The Hartree with local exchange potential is given by

$$V_{HX}(r,\theta) = \sum_{k=0,2,4} \int dr' \int d\theta' \frac{r_<^k}{r_>^{k+1}} P_0^k(\cos\theta) P_0^k(\cos\theta') \times \left[2P_{1s0}^2(r',\theta') + 2P_{2p0}^2(r',\theta') + P_{2s0}^2(r',\theta')\right] - \frac{\alpha}{2}\left(\frac{24\rho(r,\theta)}{\pi}\right)^{\frac{1}{3}}, \tag{13}$$

where

$$\rho(r,\theta) = \frac{\left[2P_{1s0}^2(r,\theta) + 2P_{2p0}^2(r,\theta) + P_{2s0}^2(r,\theta)\right]}{2\pi r^2 \sin\theta} \tag{14}$$

and the $P_{1s0}(r,\theta)$, $P_{2p0}(r,\theta)$, and $P_{2s0}(r,\theta)$ bound radial and angular orbitals are found from a molecular structure calculation [11,12] for $Li_2^+(1s\sigma^2 2p\sigma^2 2s\sigma)$ at the equilibrium internuclear distance of $R = 5.0$ for $Li_2(1s\sigma^2 2p\sigma^2 2s\sigma^2)$. Diagonalization of the $m = 0$ Hamiltonian of Eq. (7) with $\alpha = 1.10$, on a 240-point radial mesh with $\Delta r = 0.20$ and a 32-point angular mesh with $\Delta\theta = \frac{\pi}{32}$, yields an ionization potential for the $2s\sigma$ subshell of $Li_2(1s\sigma^2 2p\sigma^2 2s\sigma^2)$ of 5.11 eV, in agreement with experimental results [13].

Partial cross-section results at an incident energy of 10.0 eV, obtained by propagating the $P_{m_1m_2}^{MS}(r_1,\theta_1,r_2,\theta_2,t)$ radial and angular wave functions using Eq. (3) on a $(240 \times 32)^2$ numerical lattice with $\Delta r_1 = \Delta r_2 = 0.20$ and $\Delta\theta_1 = \Delta\theta_2 = \frac{\pi}{32}$, are presented in column 3 of Table I . The number of m_1m_2 coupled channels was 5 for $M = 0$, 6 for $M = 1$, and 5 for $M = 2$. The results presented in Table I are summed over the cross sections for $S = 0$ and $S = 1$. Separate calculations are required for each incident angular momentum l_0 as found in Eq. (6). Since partial cross sections for $-M$ are assumed equal to those for $+M$, the results presented in Table I for $M \neq 0$ are twice the individual M result.

Configuration-average distorted-wave calculations [9] were carried out for the electron-impact ionization of the $2s\sigma$

TABLE I. Partial ionization cross sections (Mb) for the electron-impact ionization of the $2s\sigma$ subshell of $Li_2(1s\sigma^2 2p\sigma^2 2s\sigma^2)$ at an incident energy of 10.0 eV (1.0 Mb = 1.0×10^{-18} cm^2).

M	l_0	TDCC ($\Delta r = 0.20, \Delta\theta = \frac{\pi}{32}$)	CADW ($\Delta r = 0.20, \Delta\theta = \frac{\pi}{32}$)	CADW ($\Delta r = 0.10, \Delta\theta = \frac{\pi}{64}$)
0	0	18.7	24.5	23.6
0	1	9.1	24.2	24.4
0	2	11.7	17.4	17.7
0	3	22.3	31.0	30.9
0	4	16.9	21.4	19.4
0	5	11.5	13.2	11.1
1	1	28.5	41.6	41.7
1	2	32.1	45.8	49.8
1	3	32.2	40.7	40.1
1	4	30.6	39.0	35.8
1	5	23.0	25.5	22.5
2	2	26.4	33.8	34.5
2	3	33.4	48.9	47.8
2	4	27.4	34.0	30.5
2	5	22.3	24.9	21.7

subshell of $Li_2(1s\sigma^2 2p\sigma^2 2s\sigma^2)$ at an incident energy of 10.0 eV. We used the same Hartree with local exchange potential found in Eq. (13) on the same $\Delta r = 0.20$ radial and $\Delta\theta = \frac{\pi}{32}$ angular mesh to generate the $P_{2s0}(r,\theta)$ bound orbital and all the $P_{klm}(r,\theta)$ distorted waves. The CADW partial cross sections are presented in column 4 of Table I. As found in Table I, the TDCC partial cross sections are lower than the CADW partial cross sections. The reduction due to electron correlation effects is in keeping with previous reductions seen in the electron-impact ionization of neutral atoms [10].

CADW calculations were also carried out for the electron-impact ionization of the $2s\sigma$ subshell of $Li_2(1s\sigma^2 2p\sigma^2 2s\sigma^2)$ at an incident energy of 10.0 eV using a $\Delta r = 0.10$ radial and $\Delta\theta = \frac{\pi}{64}$ angular mesh. Diagonalization of the $m = 0$ Hamiltonian of Eq. (7) with $\alpha = 0.63$ yields an ionization potential for the $2s\sigma$ subshell of $Li_2(1s\sigma^2 2p\sigma^2 2s\sigma^2)$ of again 5.11 eV. CADW partial cross sections for the new radial and angular mesh are presented in column 5 of Table I. Overall, the agreement between the CADW partial cross sections on the two different meshes is reasonably good. The largest disagreements are at the larger values of M and l_0, where the finer radial and angular mesh should better represent the $P_{klm}(r,\theta)$ distorted waves.

Additional CADW calculations on both radial and angular meshes were carried out for $M = 3$–4 and $l_0 = 6$–9 and extrapolated to higher M and l_0 using appropriate fitting functions [9]. The CADW total cross section at 10.0 eV on the $\Delta r = 0.20$ radial and $\Delta\theta = \frac{\pi}{32}$ angular mesh is 953 Mb, while the CADW total cross section on the $\Delta r = 0.10$ radial and $\Delta\theta = \frac{\pi}{64}$ angular mesh is 907 Mb. A TDCC total cross section is obtained by using the CADW partial cross sections on a $\Delta r = 0.20$ radial and $\Delta\theta = \frac{\pi}{32}$ angular mesh for $M \geqslant 3$ and $l_0 \geqslant 6$. The resulting TDCC total cross section at 10.0 eV is found to be 836 Mb. A TDCC total cross section is also obtained by using the CADW partial cross sections on a $\Delta r = 0.10$ radial and $\Delta\theta = \frac{\pi}{64}$ angular mesh for $M \geqslant 3$ and $l_0 \geqslant 6$. The resulting TDCC total cross section at 10.0 eV is found to be 798 Mb.

TDCC total ionization cross sections at incident energies of 10.0, 15.0, and 20.0 eV are presented in Fig. 1 . The TDCC total cross sections are "topped up" with CADW partial cross sections on a $\Delta r = 0.20$ and $\Delta\theta = \frac{\pi}{32}$ mesh and on a $\Delta r = 0.10$ and $\Delta\theta = \frac{\pi}{64}$ mesh. CADW total ionization cross sections on both radial and angular meshes at 10 incident energies between 6.0 and 25.0 eV are also presented in Fig. 1. The differences between the TDCC and CADW total cross sections are due to electron correlation effects. The differences between the CADW total cross sections are due to a better representation of large values of M and l_0.

In previous work [14], we reported CADW calculations for the electron-impact ionization of Li_2. The calculations were carried out on a $\Delta r = 0.10$–0.30 variable radial and $\Delta\theta = \frac{\pi}{64}$ angular mesh. The $P_{2s0}(r,\theta)$ radial and angular orbital for ionization was found from a molecular structure calculation [11,12] for $Li_2(1s\sigma^2 2p\sigma^2 2s\sigma^2)$. The $P_{1s0}(r,0)$, $P_{2p0}(r,0)$, and $P_{2s0}(r,0)$ radial and angular orbitals needed for the calculation of the Hartree with local exchange potential of Eq. (13) were found from a molecular structure calculation [11,12] for $Li_2^+(1s\sigma^2 2p\sigma^2 2s\sigma)$. All of the $P_{klm}(r,\theta)$ distorted waves were generated using a Hartree with local exchange potential

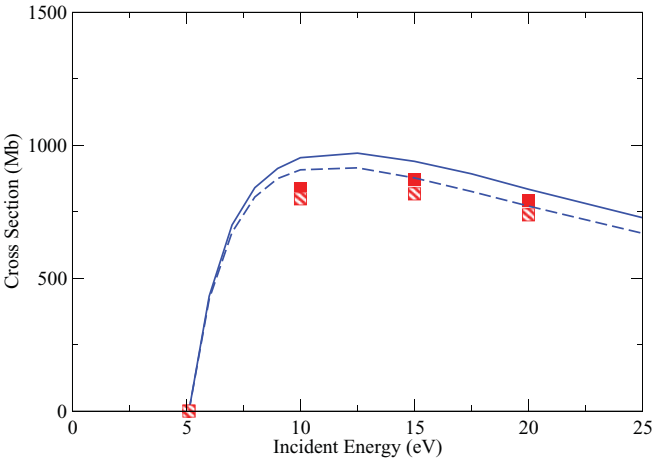

FIG. 1. (Color online) Electron-impact ionization of Li_2. Solid (red) squares, TDCC calculations "topped up" with CADW calculations on a $\Delta r = 0.20$ and $\Delta\theta = \frac{\pi}{32}$ mesh; solid (blue) line, CADW calculations on a $\Delta r = 0.20$ and $\Delta\theta = \frac{\pi}{32}$ mesh; hatched (red) squares, TDCC calculations "topped up" with CADW calculations on a $\Delta r = 0.10$ and $\Delta\theta = \frac{\pi}{64}$ mesh; dashed (blue) line, CADW calculations on a $\Delta r = 0.10$ and $\Delta\theta = \frac{\pi}{64}$ mesh (1.0 Mb = 1.0×10^{-18} cm^2).

with $\alpha = 1.0$. A total cross section around 700 Mb was found at an incident energy of 10.0 eV. We attribute the lower cross section, in comparison to the CADW results reported in this article, as due to the use of a different $P_{2s0}(r,\theta)$ radial and angular orbital in the first-order ionization matrix elements. The $P_{2s0}(r,\theta)$ radial and angular orbital from diagonalization of the Hamiltonian of Eq. (7) on a $\Delta r = 0.20$ radial and $\Delta\theta = \frac{\pi}{32}$ angular mesh has a mean radius $\langle r\rangle = 4.26$, while the $P_{2s0}(r,\theta)$ radial and angular orbital from diagonalization of the Hamiltonian of Eq. (7) on a $\Delta r = 0.10$ radial and $\Delta\theta = \frac{\pi}{64}$ angular mesh has a mean radius $\langle r\rangle = 4.29$. On the other hand, the $P_{2s0}(r,\theta)$ radial and angular orbital taken directly from a molecular structure calculation [11,12] interpolated onto a $\Delta r = 0.10$–0.30 variable radial and $\Delta\theta = \frac{\pi}{64}$ angular mesh has a mean radius $\langle r\rangle = 3.89$, making it somewhat harder to ionize. We note that the binary encounter Bethe results reported in previous work [14] had a peak cross section of 920 Mb around an incident energy of 20.0 eV.

IV. SUMMARY

In conclusion, a standard core-orthogonalization method has allowed the TDCC method to be applied to calculate the electron-impact ionization of a diatomic molecule with interior closed subshells. For the electron-impact ionization of Li_2, the nonperturbative TDCC results at the peak of the cross section were found to be lower than perturbative CADW results, in keeping with previous electron correlation effect reductions seen in the electron-impact ionization of atoms.

Although Li_2 is an ideal system to study due to its tight $1s\sigma^2 2p\sigma^2$ inner core, the CADW cross sections are found to be sensitive to the choice of the valence orbital for the $2s\sigma$ subshell. Due to the absence of experiment, we plan further nonperturbative TDCC calculations with different valence orbitals in pursuit of a

truly benchmark electron-impact ionization cross section for Li_2.

In the future, we also plan to apply the TDCC method to the calculation of the electron-impact ionization of other diatomic molecules, like C_2 and CO. Besides total cross sections, energy and angle differential cross sections can be extracted using the fully propagated $P^{MS}_{m_1m_2}(r_1,\theta_1,r_2,\theta_2,t \to \infty)$ radial and angular wave functions. We also note that the use of a core-orthogonalization method allows the electron-impact ionization of the inner subshells of both atoms and molecules that possess outer closed subshells.

ACKNOWLEDGMENTS

This work was supported in part by grants from the US Department of Energy. Computational work was carried out at the National Energy Research Scientific Computing Center in Oakland, CA.

[1] J. D. Gorfinkiel and J. Tennyson, J. Phys. B **38**, 1607 (2005).
[2] E. Krishnakumar and S. K. Srivastava, J. Phys. B **27**, L251 (1994).
[3] H. C. Straub, P. Renault, B. G. Lindsay, K. A. Smith, and R. F. Stebbings, Phys. Rev. A **54**, 2146 (1996).
[4] M. S. Pindzola, F. Robicheaux, and J. Colgan, J. Phys. B **38**, L285 (2005).
[5] M. S. Pindzola, F. Robicheaux, S. D. Loch, and J. P. Colgan, Phys. Rev. A **73**, 052706 (2006).
[6] B. Peart and K. T. Dolder, J. Phys. B **6**, 2409 (1973).
[7] J. Colgan, M. S. Pindzola, F. Robicheaux, C. Kaiser, A. J. Murray, and D. H. Madison, Phys. Rev. Lett. **101**, 233201 (2008).
[8] J. Colgan, O. Al-Hagan, D. H. Madison, C. Kaiser, A. J. Murray, and M. S. Pindzola, Phys. Rev. A **79**, 052704 (2009).
[9] M. S. Pindzola, F. Robicheaux, J. Colgan, and C. P. Ballance, Phys. Rev. A **76**, 012714 (2007).
[10] M. S. Pindzola *et al.*, J. Phys. B **40**, R39 (2007).
[11] Theoretical Chemistry Group, Computer code ALCHEMY (IBM Research Laboratory, San Jose, CA, 1970).
[12] M. A. Morrison, Comput. Phys. Commun. **21**, 63 (1980).
[13] [http://physics.nist.gov/PhysRefData].
[14] M. S. Pindzola, F. Robicheaux, C. P. Ballance, and J. Colgan, Phys. Rev. A **78**, 042703 (2008).